Chapter 5

Electric and Thermal Operations of Furnaces for Ferroalloys Production

Gudrun Saevarsdottir
Reykjavik University, Reykjavik, Iceland

Chapter Outline

5.1 INTRODUCTION TO FURNACE OPERATIONS FOR FERROALLOYS PROCESSING

Ferroalloys are produced in several types of furnaces, depending on the chemistry as well as the thermal and electrical parameters of the specific process. The

Handbook of Ferroalloys. http://dx.doi.org/10.1016/B978-0-08-097753-9.00005-8

most used are submerged arc furnaces (SAFs) and resistance-heating furnaces (RHFs), where heating of the charge, slag, and alloy proceeds by the application of electric current. In these electric furnaces, the tips of electrodes protrude into the furnace hearth and become hidden by a burden (charge) of raw materials, which have been fed into the furnace from the top. The burden typically is partially transformed by chemical reactions appropriate for the respective reaction zones in the furnace at the local temperature and pressure. The main difference between SAFs and RHFs is whether or not an electric arc is present at the tip or along the side of the electrode. For example, in silicon and ferrosilicon production, the temperature required for the process to run with an acceptable silicon yield is above 1900°C. This requires an intense heat source and therefore dictates the formation of an electric arc, rather than heating by ohmic resistance (joule heating). The latter proceeds when electric current is conducted through the charge or slag surrounding the electrodes. Several ferroalloys smelting processes do not require an arc in order to reach the necessary thermodynamic conditions, but in many cases there are strong indications that an arc may nevertheless be present, such as in ferrochromium or ferromanganese production.

As the sole purpose of the electric current passing through the SAF is to release heat to fuel the chemical processes in the furnace, the current can be either AC or DC. The most common configuration for an industrial scale furnace is three-phase AC, where three electrodes are embedded into the furnace raw material charge. Three AC-current phases separated by a phase shift of 120° pass through the respective electrodes and cancel out at a star point located in the center of the furnace. One phase AC is used mostly in smaller laboratory or pilot scale furnaces, and it requires a top and a bottom electrode. DC furnaces also require a bottom electrode in addition to the consumable electrode from the top. Both small scale and large industrial scale DC furnaces are in operation around the world.

An extensive description of the design of SAFs and RHFs, along with the associated subprocesses, is presented in Chapter 4. This chapter describes in more detail the electrical operation of the furnace with the goal of creating the optimal thermal conditions, and it provides a complementary analysis of the environmental effects.

Before addressing the electric particularities for different furnace designs, a brief introduction to electric circuit theory as relevant to understand the furnace circuit is given. Even though electric arcs will distort the sinusoidal current and voltage waveforms, for practical purposes of furnace circuit analysis this will be minimal and the treatment described here can be considered generic and applicable to all submerged arc furnaces.

5.2 BASICS OF ELECTRIC CIRCUIT THEORY

5.2.1 Direct and Alternating Current and Voltage

Any electric network consists of electrical elements such as voltage and current sources, resistors, inductors, capacitors, transmission lines, switches,

transformers, and other electrical equipment. An electric circuit is an electric network where all components are connected into a closed system so that the current will have a return path (Schultz, 2006). Real electrical systems show complicated responses to different types of current and voltage input because of the formation of electric and magnetic fields. The properties of electric systems that can be attributed to these physical phenomena are called reactance. In the analysis of real circuits, a simplifying assumption is made by assuming that these properties are lumped into simple electrical elements such as inductors and capacitors.

Electric current is the flow of electric charge through a conductive medium and has the units of charge pr. time unit. The SI unit for electric current is ampere (A), which is equivalent to 1 coulomb of charge passing per one second. Time invariant current is called direct current (DC). A common convention for DC current, which is applied here, is to denote the current by I. A periodic, time-dependent current, where the flow of moving charges is periodically reversed, is termed alternating current (AC). The most commonly applied AC form is using a periodic sinusoidal form. Other AC current waveforms occur in special applications, but a sinusoidal AC waveform is the form in which electric power is produced and delivered to homes and businesses, and this type of current is considered further in this chapter (Schultz, 2006). Deviations are due to nonlinear components such as the electric arcs found in submerged arc furnaces.

Sinusoidal AC and voltage can be written as

$$i(t) = I_0 \sin(\omega t + \varphi_i), \qquad u(t) = U_0 \sin(\omega t + \varphi_u), \tag{1}$$

where t is time, I_0 and U_0 are the maximum values (amplitude) of current and voltage, ω is the angular frequency derived from the frequency f of the AC ($\omega = 2\pi \cdot f$), and ϕ_i and ϕ_u are the phase angles for the current and voltage, respectively, and describe current and voltage values at zero time (Fig. 5.1). The period of AC repetition is $\tau = 1/f$ (e.g., for 50 Hz frequency of standard electricity supply, the period of one oscillation will be 20 ms). In resistive circuits that have no reactance, the phase angles are identical for current and voltage. In the presence of unbalanced reactance, they are not, as the voltage is phase-shifted with respect to the current.

The $i(t)$ and $u(t)$ are the real current and voltage values as a function of time. In the analysis of electrical circuits, it is convenient for mathematical purposes to use complex notation to describe the cyclic circulation of i and u. As harmonic functions are often represented in circular form, a vector corresponding to an instant value of either current or voltage might be written using Euler's formula:

$$i(t) = I_0(\cos(\omega t + \phi_i) + j\sin(\omega t + \phi_i)) = I_0 e^{j(\omega t + \phi_i)}, \tag{2a}$$

$$u(t) = U_0(\cos(\omega t + \phi_u) + j\sin(\omega t + \phi_u)) = U_0 e^{j(\omega t + \phi_u)}, \tag{2b}$$

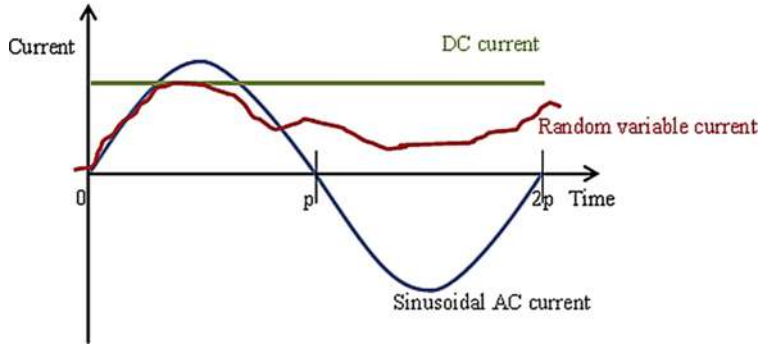

FIGURE 5.1 Examples of DC, sinusoidal AC (with a period of $2p$), and random current plots.

where $j^2 = -1$ is the imaginary unit. The imaginary parts of the current and voltage do not have a physical manifestation, but they are defined to simplify the mathematical analysis of the system (Schultz, 2006). They allow current and voltage to be displayed in a form of so-called phasors, as illustrated in Figure 5.2. When phase shifts of current and voltage are different, current and voltage vectors are rotating with a constant angle difference between them (Fig. 5.3).

The acting value of current and voltage, also known as the root mean square (RMS) value, is defined as an integral of half-period divided by the half-period

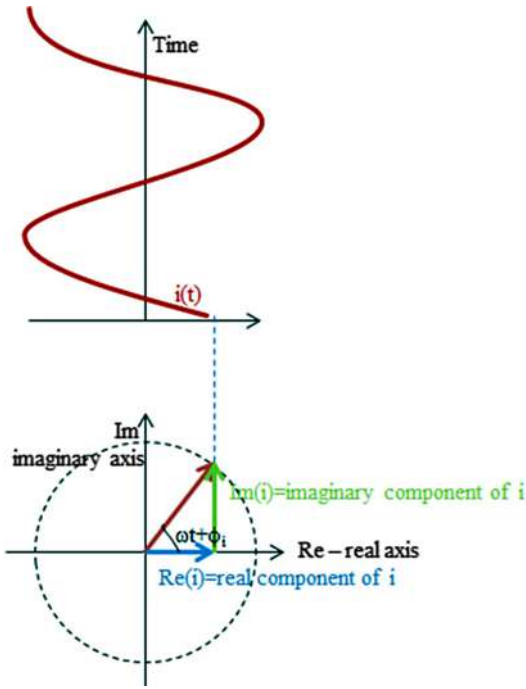

FIGURE 5.2 Illustration of a phasor representation of AC with a sinusoidal waveform.

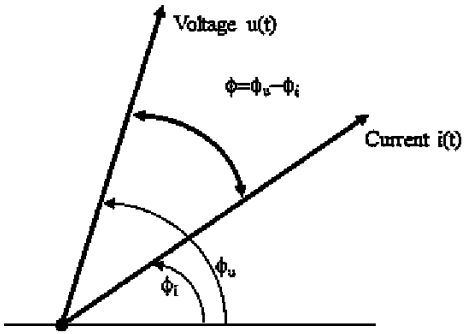

FIGURE 5.3 Illustration of the phase angle difference between AC and voltage.

time (p; see Fig. 5.1), which for a sinusoidal waveform is $U_{RMS} = U_0/\sqrt{2}$, $I_{RMS} = I_0/\sqrt{2}$. Using this RMS value it is possible to denote the relation between alternative current, voltage, and power in a way that is analogous to the DC representation. Another more compact shorthand notation of the Euler representation of the current and voltage is $i(t) = I_{RMS} \angle \phi_i$, $u(t) = U_{RMS} \angle \phi_u$.

5.2.2 Resistive Circuits

The simplest form of an electric circuit is the resistive circuit, which contains a power source and a resistance R but no reactance. The SI unit for a resistance is Ohm (Ω). The voltage drop over the resistance is simply $U_{RMS} = I_{RMS} \cdot R$, and the power dissipated to heat in the resistance is $P = U_{RMS} \cdot I_{RMS} = R \cdot (I_{RMS})^2$. A purely resistive circuit will in the AC case not affect the phases of the current and voltage ϕ_i and ϕ_u, so the current and voltage over a pure resistance will be in phase with one another $u(t) = i(t) \cdot R$.

5.2.3 Reactance Circuits

Inductive reactance appears as a result of the energy stored in a magnetic field and released from this field, caused by current flowing through the circuit. Inductance is denoted by L and the SI unit is henry (H). The voltage over the self-inductance in a circuit is proportional to the rate of change in the current or more specifically the derivative of the current with proportionality constant L:

$$u(t) = L\frac{di(t)}{dt}. \tag{3}$$

In the case of DC, which is time invariant, no voltage is associated with inductance, as the DC time derivative is zero by definition. For AC, however, the complex representation will give the following form:

$$u(t) = L\frac{di(t)}{dt} = jL\omega \cdot i(t). \tag{4}$$

Comparing this equation with the one presented earlier for pure resistance, it might be assumed that the combination of parameters L, frequency ω and imaginary unit j, linking voltage and current has the same meaning of resistance as for R. However, in this case it is frequency-dependent inductive resistance $X_L = \omega L$. The RMS voltage over an inductance is therefore written as $U_{RMS,L} = jX_L \cdot I_{RMS}$

As follows from the representation of phasors (see Figs 5.2 and 5.3), the multiplier j means that the voltage vector would be ahead of the current vector by 90° (+ π/2). The same might be also seen as delayed current: when voltage over inductance changes, the current is delayed by 90°C because of the inevitable creation of a magnetic field in inductance, which stores energy. This energy is purged back to the circuit in the next half-period (Schultz, 2006).

Electric capacitance is the ability of a system to store electric charge. In the case of a parallel plate capacitor, the capacitance is proportional to the area of the plates and inversely proportional to the distance between them. If the charges on the plates are $+Q$ and $-Q$ and U is the voltage between the plates, the capacitance C is given by $C = Q/U$. The capacitance has the SI unit farad (F). Capacitative reactance appears because of the energy stored in the electric field formed by the charges collected on the capacitor plates (for inductance it was a magnetic field). The stored charge is proportional to the integral of the current applied to it over the half-period time (charging), so the relation between current and voltage over a capacitor with capacitance C becomes

$$u(t) = \frac{1}{C}\int_0^p i(t)dt. \tag{5}$$

In reality, an accumulated electric charge does not pass through a capacitor (Schultz, 2006). For AC current, the charges will just oscillate between the parallel plates of the capacitor, but a DC current will not pass through it. Therefore, a capacitance functions as a circuit breaker unit for DC. For AC however, the complex representation of the integral will give the following form of the equation:

$$u(t) = \frac{1}{C}\int i(t)dt = -\frac{j}{\omega C}i(t). \tag{6}$$

Similar to the resistance and inductance, here the capacitative reactance may be defined as

$$X_C = -\frac{1}{\omega C} = -\frac{1}{2\pi f C}. \tag{7}$$

Respectively, the RMS voltage over a capacitor is $U_{RMS,C} = jX_c \cdot I_{RMS}$, but X_C has negative sign as opposed to X_L. So for the inductance, the voltage over a capacitance is phase-shifted by +90° from the current, but in the case of the

capacitance, the voltage lags -90° ($-\pi/2$) behind the current. This might be seen as the delayed voltage rise over a capacitor, because at some applied current some time is needed for charges to accumulate and the capacitor to be charged, and this electric energy storage delays rising of the voltage.

The total reactance in a circuit is a combination of the inductive (X_L) and capacitative (X_C) reactances:

$$X = X_L + X_C = \omega L - \frac{1}{\omega C}. \tag{8}$$

Note that the capacitative reactance is subtracted from the inductive reactance. This is a very important feature, which is systematically utilized in the design of electric power systems, as a method to compensate for inductive reactance and minimize the reactance of the system (Schultz, 2006).

5.2.4 Impedance and Power in AC Circuits

The total impedance, denoted by Z, describes the opposition from a circuit to the passage of current given an applied voltage, which as follows from Ohm's law is $Z = U_{RMS}/I_{RMS}$. The impedance is a combination of the reactance and the resistance in a circuit: $Z = R + jX$. Thus, impedance is a complex parameter and the two components, resistance (active) and reactance (reactive), are orthogonal in the complex plane. As any complex variable, it can also be characterized by its length $|Z|$ and the angle ϕ:

$$Z = R + jX = |Z|e^{j\phi}, \quad |Z| = \sqrt{R^2 + X^2}, \quad \phi = \arctan(X/R). \tag{9}$$

From this definition it follows:

$$U = (R + jX)\cdot I = (R + j\omega L - j\frac{1}{\omega C})\cdot I = |Z|Ie^{j\phi} \tag{10}$$

or for current and voltage in the complex formulation:

$$U_0 e^{j(\omega t+\phi_u)} = |Z|e^{j\phi}\cdot I_0 e^{j(\omega t+\phi_i)} = |Z|I_0 e^{j(\omega t+\phi_i+\phi)}, \quad \phi = \phi_u - \phi_i \tag{11}$$

The angle shift ϕ determined by the ratio of R and X is the phase angle between current and voltage in the circuit (see Fig. 5.3), leading up to the important concept of the power factor. The relation between total impedance Z, resistance R, and reactance X is shown schematically in Figure 5.4 together with corresponding voltage drops (Hochrainer, 1970).

As Figure 5.4 shows, voltage drop over capacitance is subtracted from the voltage drop over inductance, and their difference is the reactance voltage, which does not contribute to active heating. The power dissipated as heat in a circuit is the product of the current through a resistance I_{RMS} and the voltage over the resistance $U_{RMS} = I_{RMS}\cdot R$. The voltage over the whole circuit also includes the voltage over the reactance, so instead of the real power, the product of the instant, time-dependent voltage and current gives the apparent power

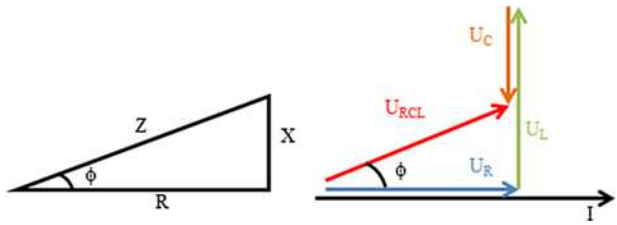

FIGURE 5.4 Phasor representation showing the impedance in a circuit and corresponding voltages over the different component types.

$s(t) = u(t) \cdot i(t)$. Expanding the harmonic functions of voltage and current and rearranging the real terms allows writing the expression for $s(t)$ as

$$\begin{aligned} s(t) &= u(t) \cdot i(t) = \frac{U_0 I_0}{2} (\cos(\phi) \cdot (1 - \cos(2\omega t) + \sin(\phi) \cdot \sin(2\omega t)) \\ &= p(t) + q(t). \end{aligned} \tag{12}$$

The first term $p(t)$ of the expression is always positive and is called real (or active) power; the second term has a time-averaged value zero and is termed reactive power $q(t)$. The reactive power represents energy, which is stored in electric and magnetic fields and swings back and forth in the system at every period without doing any useful work. The mean value of the real power term can be expressed as

$$P = \frac{U_0 I_0}{2} \cos(\phi) = U_{RMS} \cdot I_{RMS} \cdot \cos(\phi) \tag{13}$$

Therefore, this equation has the same form as for the power in a DC circuit apart from the additional power factor $\cos(\phi)$, which is a very important parameter for all AC electric power systems. Figure 5.5 shows the current and voltage and the apparent power $s(t)$ in two cases: with no reactance and no phase shift between current and voltage, and with some phase shift (Hochrainer, 1970).

In the first case ($\phi = 0$), the apparent power always has a positive value. When phase shift is nonzero, the apparent power will take negative values during those time intervals where current and voltage have different signs. This means that at negative apparent power, the reactance in the circuit is returning the reactive power previously stored as energy in electric or magnetic fields.

Similar to real power, the acting value of the reactive power could be written as $Q = U_{RCL,\,RMS} \cdot I_{RMS} \cdot \sin(\phi)$. Apparent, real, and reactive power functions may also be represented in a complex plane as a vector diagram, in the same way as for current and voltage. The average (acting) apparent power is $\overline{S} = \overline{U}_{RCL,RMS} \cdot \overline{I}^{*}_{RMS} = P + jQ = S \angle \phi$. The apparent power is expressed in volt-amperes (VA) and the reactive power in volt-ampere reactive (VAr), to differentiate it from real power, which is always expressed in watts (W). In submerged arc furnace design, the electric equipment for the furnace must be designed with a capacity for both the reactive power and the real power.

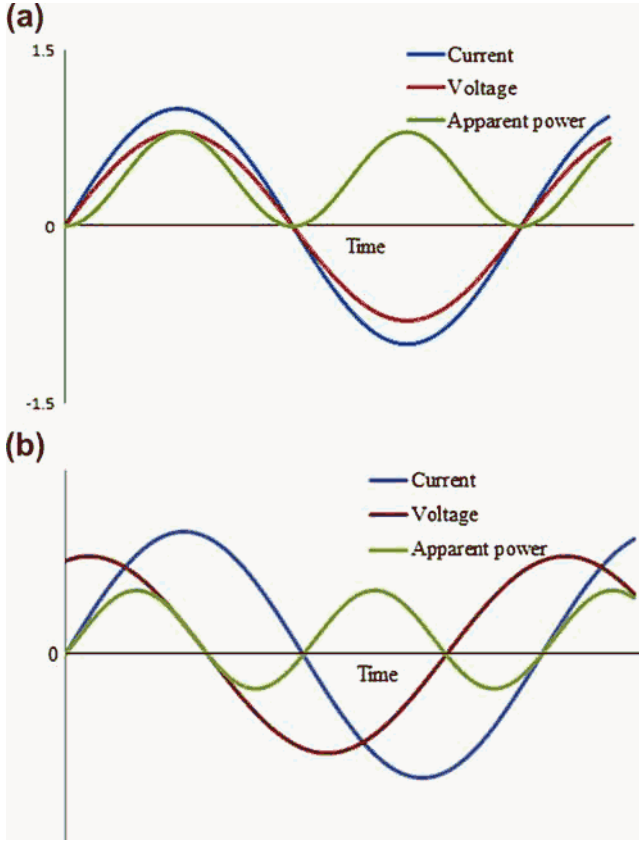

FIGURE 5.5 Apparent power for a real circuit where there is no phase shift between current and voltage (a) and with a phase shift of ϕ between current and voltage (b).

5.3 FERROALLOY SMELTING FURNACES AS ELECTRICAL CIRCUITS

5.3.1 DC Furnaces

The electric circuit and an associated load curve for DC furnaces allow for the simplest description of circuit and characteristics on the secondary side ("short net"; see Chapter 4), after the power rectifying equipment. A simplified schematic of the electric circuit for a DC furnace is shown in Figure 5.6.

The current in the circuit is $I = U_0/(R_{int} + R_{load})$, where R_{int} is internal resistance of the circuit itself, R_{load} is the load (useful) resistance, and U_0 the voltage delivered by the rectifying equipment on the secondary side. Respectively, the power over the load-bearing resistance is

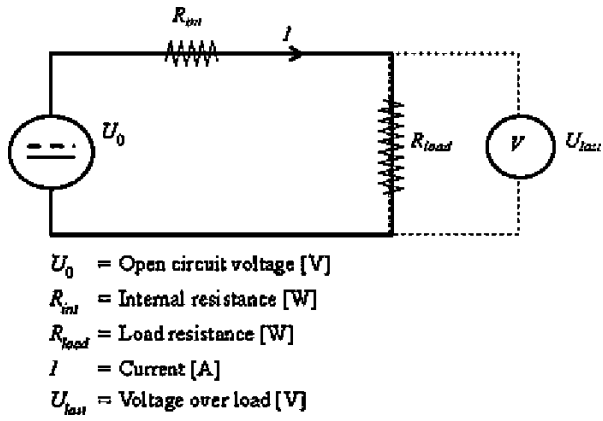

FIGURE 5.6 Schematic illustration of a DC furnace circuit.

$$P = R_{load} \cdot I^2 = \frac{R_{load} \cdot U_0^2}{(R_{int} + R_{load})^2}. \tag{14}$$

Maximum power is theoretically obtained when $R_{load} = R_{int}$, with values for voltage and current as $U_{load} = U_0/2$, $I_m = U_0/(2R_{int})$ and $P_m = U_0^2/(4R_{int})$. An attractive feature of DC furnaces is that inductance, which leads to a lowering of the power factor in large AC furnaces, does not have a similar effect in DC. Therefore, large furnaces supporting high currents can be designed without concern for low power factor and phases interaction, complicating the electrode control operations. Also, the absence of a skin effect and proximity effect enables a more efficient utilization of the whole electrode cross-sectional area for current conduction. There are furnace producers that have designed industrial DC furnaces where the location and movement of the electric arc is controlled by external magnetic fields. The main disadvantage of the DC furnace, apart from expensive rectifying equipment for converting low-voltage AC to DC, is the necessity of the bottom anode. The bottom anode is a critical and sensitive part of the DC furnace design.

5.3.2 AC Furnaces

Most industrial AC furnaces are of the three-phase type, with three or six consumable electrodes penetrating the furnace charge from above, each carrying separate phases that are phase displaced by 120° from one another. For six-electrode furnaces; the phases are directed to every pair of the electrodes (Valderhaug, 1992). Also, smaller one-phase AC furnaces exist on laboratory or pilot scales (e.g., Larsen, 1996).

The currents from the three phases cancel out at a star point within the furnace, and no bottom electrode is required. When discussing the electrical characteristics of AC furnaces, it is useful to make a simplifying analogy with

a one-phase circuit, which is justified for a symmetric configuration. For a one-phase AC furnace following analyses I and U, always refer to RMS values (i.e., $I = I_{RMS}$ and $U = U_{RMS}$).

5.3.2.1 One-Phase AC Circuit

Figure 5.7 is a schematic of a one-phase AC furnace circuit. The resistances in the system are divided into two resistances based on their usefulness. The load resistance R_ρ in this case is the lumped resistance in the charge and eventual electric arc. The heat dissipated by the current running through the load resistance represents the useful power, which supplies heat needed for the chemical reactions in the furnace.

Resistance in the outer circuit serving the furnace as well as the resistance in the upper part of the electrode are not in use for the process and therefore termed as a loss resistance r. The real power in the furnace is $P = I^2(R_r + r)$.

A typical SAF has relatively low voltage and high currents, and therefore a considerable magnetic field is generated around the electrodes, conductors, and other equipment. A significant amount of energy is stored in this magnetic field and is pumped in and out of the circuit as the current alternates. This reactive power Q_L causes a phase shift between the current and voltage in the system. The associated lumped reactance $X_L = \omega L$ is a characteristic of the furnace and is distributed all through the furnace and current carrying equipment rather than concentrated in a coil. In the simplified schematic of the circuit it is, however, substituted by a representative coil with an inductance L. There is very little capacitance on the secondary side of the furnace, and eventual capacitive reactance is usually neglected and the total reactance is $X = X_L$. The current in the circuit is calculated from the voltage delivered to the circuit:

$$I = \frac{U_2}{Z} = \frac{U_2}{\sqrt{X^2 + R^2}}. \tag{15}$$

The voltage share caused by the reactance is proportional to the derivative of the current and is therefore for a sinusoidal current source phase-shifted by $+90^\circ$ from the voltage over the resistance that is in phase with the current. The overall voltage is a combination of the real voltage and the reactive voltage and is therefore phase-shifted by an angle ϕ with regard to the current. This phase shift increases with increased reactance in the furnace circuit (see Fig. 5.5).

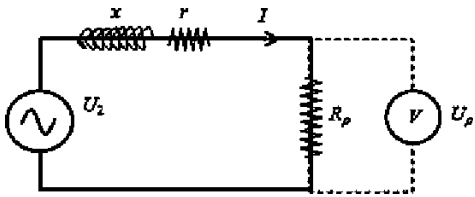

FIGURE 5.7 Schematic of a one phase AC circuit as discussed in this section.

Total active power P [kW], reactive power Q_L [kVAr], and apparent power S [kVA] depend on the resistance R as follows:

$$P = R\,I^2 = \frac{R{U_2}^2}{X^2 + R^2}, \quad Q_L = X\,I^2 = \frac{X{U_2}^2}{X^2 + R^2}, \quad S = \sqrt{P^2 + {Q_L}^2}. \tag{16}$$

The real furnace power P can be also expressed in terms of the power factor $\cos(\phi)$ as $P = S{\cdot}\cos(\phi)$, or in terms of current as $P = \sqrt{S^2 - {Q_L}^2} = \sqrt{U_2^2 I^2 - X^2 I^4}$. The useful power P_ρ, which is explicitly developed in R_ρ and released as heat in the charge and the arc, is

$$P_\rho = R_\rho I^2 = \frac{R_\rho U_2^2}{X^2 + (R_\rho + r)^2}. \tag{17}$$

The maximum total active power in the furnace is obtained for $R = R_\rho + r = X$ and it is equal to

$$P_m = \frac{U_2^2}{2X} \tag{18}$$

with the current at this full load point,

$$I_m = \frac{U_2}{\sqrt{2}X}, \tag{19}$$

and the charge voltage $U_\rho = R_\rho I$. The circuit loss resistance r might be measured with the electrode lowered in the furnace so that it reaches direct contact with the bottom electrode and the charge is short circuited ($R_\rho = 0 \rightarrow R = r$). The associated short circuit current is

$$I_s = \frac{U_2}{\sqrt{X^2 + r^2}} = \sqrt{\frac{2X^2}{X^2 + r^2}} I_m \tag{20}$$

and impedance is $Z_k = \sqrt{X^2 + r^2}$. It is easily shown that the maximum useful charge power is achieved when $R_{\rho m} = Z_k$ leading to the maximum charge power and the current:

$$P_{\rho m} = \frac{Z_k U_2^2}{X^2 + (Z_k + r)^2}, \qquad I_m = \frac{U_2}{\sqrt{X^2 + (Z_k + r)^2}}. \tag{21}$$

For very low loss resistance ($r << X$), $Z_k \approx X$ and, respectively,

$$I_{sc} = \frac{U_2}{X} = \sqrt{2} I_m, \qquad P_{\rho m} = P_m = \frac{U_2^2}{2x}, \qquad I_{\rho m} = I_m = \frac{U_2}{\sqrt{2}X}. \tag{22}$$

With these, the most important parameters of a one-phase AC furnace, it is possible now to address the three-phase AC furnace.

5.3.2.2 Three-Phase AC Furnace

The standard Knapsack connection for a three-phase furnace is shown in Figure 5.8. One three-phase transformer or three single-phase transformers are coupled in a delta connection and are attached to the furnace electrodes at the same point where each pair of transformers is connected to one another.

The electrodes form a star circuit with a floating neutral point (zero point) where the sum of the instantaneous currents is zero: $i_1+i_2+i_3=0$. The complete three-phase circuit is shown in Figure 5.9. As the figure shows, the reactance in the furnace is distributed into inductances in the respective phases and also in the triangular delta connection.

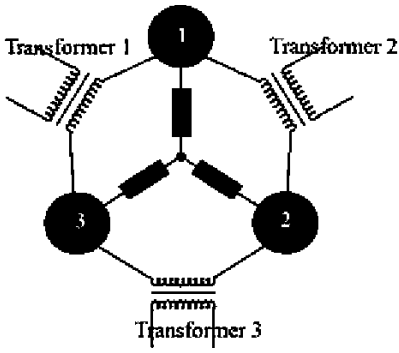

FIGURE 5.8 Three symmetrically configured one-phase transformers in a Knapsack connection with the three electrodes connected at a floating star point.

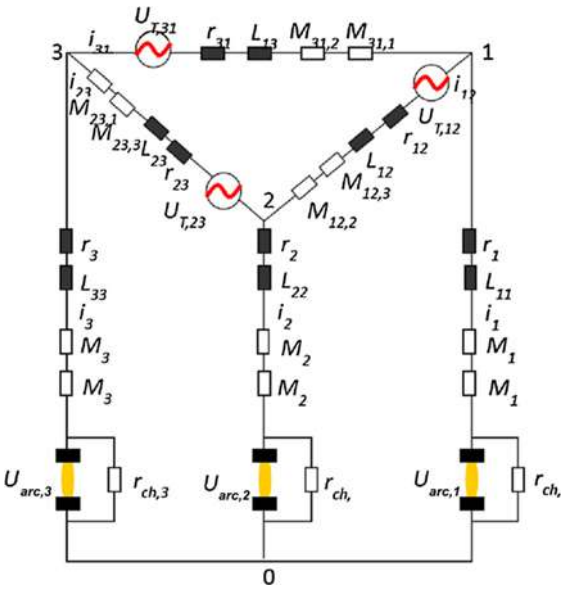

FIGURE 5.9 A schematic of a complete three-phase AC-furnace circuit with resistances, reactances, and mutual reactances shown as lumped circuit elements.

On the secondary side of the transformer windings there is no capacitance, so there reactance is only due to inductances L_{12}, L_{23}, and L_{13}, hence there $X = X_L$. Also, the presence of mutual inductances ($M_{ij,k}$) should be noted—they represent the induced voltage in a phase, due to the magnetic field generated by the current passing through the other two phases. This property of the three-phase circuit turns out to be quite important in the furnace operation, as it represents an interaction between the phase currents, which complicates the electric control of the furnace. A change in the current passing through one phase affects the current passing through the other two (Valderhaug, 1992). This phenomenon is further discussed when the electric operation of the furnace is addressed.

In the case of a symmetric furnace operation, the three-phase furnace circuit can be simplified into three one-phase equivalent circuits, where the currents are decoupled from one another and resistance and reactance have been merged into their lumped counterparts (see Fig. 5.7). The mutual inductances $M_{ij,k}$ are lumped into the phase inductance L_k, which can be justified when all conditions are symmetric. The delta-connected secondary voltage here is replaced by line voltages $u_{Tij} = U_2/\sqrt{3}$. Thus, the open-circuit voltages of the transformer secondaries have equal RMS values and a 120° phase delay between them. In this context, R is then termed *phase resistance* and X the *phase reactance,* both usually written in units of mΩ. For these conditions, the phase current is

$$I = \frac{1}{\sqrt{3}} \frac{U_2}{\sqrt{X^2 + R^2}}, \tag{23}$$

the furnace real power is

$$P = 3 \cdot R I^2 = \frac{R \cdot U_2^2}{X^2 + R^2}, \tag{24}$$

and the reactive power is

$$Q_L = 3 \cdot X I^2 = \frac{X \cdot U_2^2}{X^2 + R^2}. \tag{25}$$

As for one-phase AC furnaces, the active power in the furnace can be written in terms of the transformer secondary voltages and phase current: $P = \sqrt{3U_2^2 I^2 - 9X^2 I^4}$. The useful power dissipation in the furnace charge is

$$P_\rho = 3 \cdot R_\rho I^2 = \frac{R_\rho U_2^2}{X^2 + R^2} \tag{26}$$

with the apparent power $S = \sqrt{3}\, U_2 \cdot I$, $S = P/\cos(\phi)$. The reactance X in an SAF increases with increasing furnace size and phase current. Large industrial furnaces of 40 to 50 MVA may have a reactance that substantially surpasses the resistance, leading to a relatively low power factor of less than 0.6.

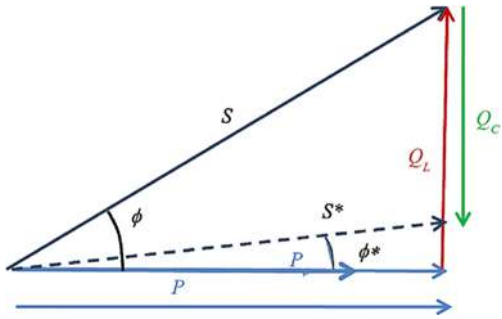

FIGURE 5.10 A vector diagram illustrating how capacitative compensation on the primary side of the transformer windings is used to swallow the reactive power and elevate the power factor. This is done at SAF facilities to meet the requirements of the power distribution utility.

Even though the power factor cannot be compensated on the secondary side, it must be on the primary side. As most of the reactance is inductive, it can be compensated by arrangements of capacitor batteries, which deliver their reactive power on the low-current primary side of the delta connection. This is necessary to protect the transport grid from the power factor and satisfy predetermined criteria from the power distributor (Schultz, 2006). Properly designed capacitor compensation can increase the power factor toward unity as seen from the grid. This is illustrated in a vector diagram in Figure 5.10.

It is not practical to compensate with capacitance on the high current secondary side of the transformers, and therefore the whole furnace circuit must be designed with extra capacity to accommodate for an apparent power *S,* which greatly exceeds the active power *P.* Also the induced fields in the furnace complicate the electrode operation associated with the electric control, as will be discussed in Section 5.5.

5.4 MODES OF HEAT DISSIPATION IN FURNACES

There are two main modes of heat dissipation in ferroalloys smelting furnaces. All furnaces have a part of the electrode current passing through the charge burden, molten slag, and metal. This will involve resistance heat dissipation, also called joule heating. In some processes, an electric arc will also be present, with a significant part of the heat dissipation. This is required for some types of the processes depending on the need for a high-temperature heat source for the chemical reactions, although arcing might be also found in other cases where it is not specifically required.

5.4.1 Electric Arc

An electric arc is formed when high electric field strength (voltage gradient) over normally nonconductive material, such as a gas, causes an electric breakdown of the material, which increases the conductivity in the medium. In the case of arc discharge for a gas, the ionization of the gas molecules introduces positively charged ions and electrons that enable electric current to pass through

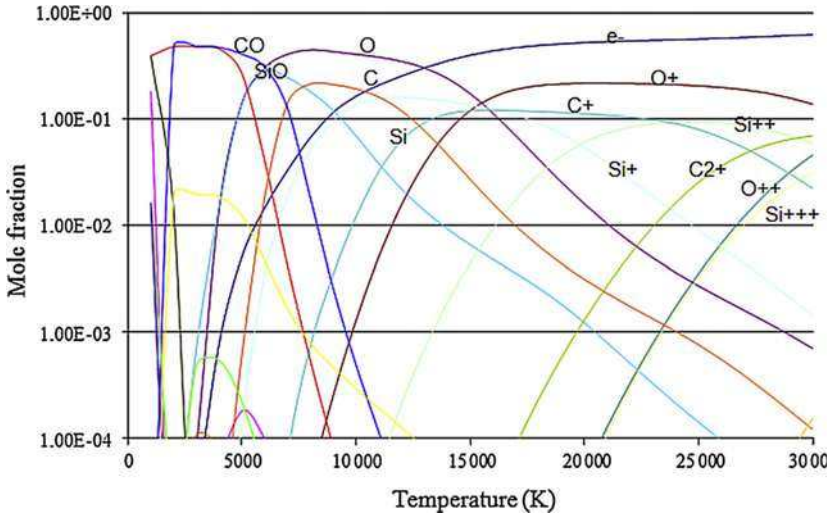

FIGURE 5.11 Density of different species present in a gas composed of Si-O-C plasma of 1:2:1 composition, as can be found in the crater of a Si-producing electric arc. In this gas mixture, some Al and Ca contaminant (not shown here) are present (Saevarsdottir et al., 2001b)

the medium. The ionized gas (plasma) is generally defined as a special state of matter in addition to solid, liquid, and gaseous states. Electric arcs in SAFs are formed at atmospheric pressure, which requires the formation of thermal plasma, which means that ions and electrons have the same kinetic energy (Chen, 1990). In less dense plasmas, electrons may be at a higher temperature than the heavy particles. For air and most other gases, the temperatures required for sufficient ionization for thermal plasma formation are above 8000 K.

As an example, Figure 5.11 shows the density of species as a function of temperature in a Si-O-C plasma (molar ratio Si:O:C = 1:2:1), which is the approximately expected gas composition in the crater of a silicon smelting furnace). A commonly faced arc temperature in an SAF is above 20 000 K, which means that heat released in the arc can support reactions requiring extremely high temperatures to run.

An industrial arc with a voltage of 100 V would typically not be much longer than 10 cm, and there may be more than one arc burning in parallel from the same electrode (Reynolds, 2011). Figure 5.12 shows a photograph of a 5-cm-long low current DC arc (2000 A) with a normal polarity where the top electrode is cathode (a) and a photograph of three arcs burning in parallel (b). (Courtesy of R. Jones and Q. Reynolds, Mintek, South Africa.)

The electromagnetic forces in the arc acting on the plasma are the strong drivers for fluid flow, so velocity of the plasma from the cathode toward the anode in the arc is high and pressure at the anode end is significant. Velocities can approach sonic speed, even though the sound velocity is much higher for

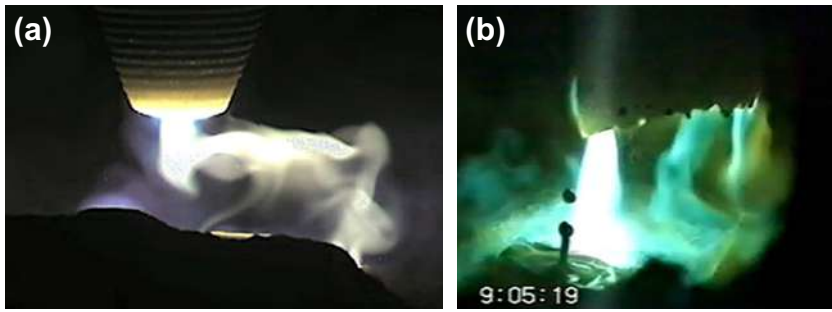

FIGURE 5.12 Photographs of (a) a 5-cm-long low-current (2000A) DC arc with a normal polarity where the top electrode is cathode and (b) three arcs burning in parallel. *(Courtesy of Q.G. Reynolds and R. Jones, Mintek, South Africa.)*

thermal plasma than for air at standard conditions. The heat released in the arc due to resistive dissipation, $P_a = R_a \cdot I^2$, is transported from the arc to its environment mainly through convection and radiation approximately equally distributed (Saevarsdottir et al., 2001a). However, a significant fraction of the heat is also delivered to the anode with particles impacting its surface (Palsson et al., 2007) as well as through proximity radiation, so the anode will receive a significantly more substantial heat load as compared to the cathode.

Although the electric arc serves as a resistive heat dissipater in the furnace, it has some characteristics that separate it from normal resistors. Primarily its resistance is nonlinear, as it depends on the current that passes through it. Therefore, the arc resistance varies over the 20 ms AC period (at 50 Hz frequency), being highest when the current passes through zero and lowest when the current passes through the sinusoidal maximum. As the temperature required for full ionization in the plasma is very high, the level of cooling and the temperature of the surrounding environment will affect the characteristics of the arc. When the current passes through zero, the heat dissipation by the current passing through the arc will not be sufficient to balance the heat loss by radiation and convection. Colder environments will lead to a higher variation in the arc resistance within the arc period, increasing the nonlinear properties of the electric arc. Figure 5.13 shows how the arc voltage dynamics will qualitatively change over a half period depending on the temperature of the surroundings, assuming that the current is imposed with a sinusoidal waveform.

In the case of large submerged arc furnaces, a high inductance will ensure a sinusoidal current waveform and nonlinearity will be reflected in the voltage waveform. Figure 5.14 shows the dynamic current-voltage characteristics for this same case (the so-called Lissajous curve).

This nonlinearity gives rise to harmonics in the voltage and current waveforms of the SAF, which can be utilized to deduce the level of arcing in the furnace. An example for a silicon smelting furnace is shown in Figure 5.15 during a period of charge smelting.

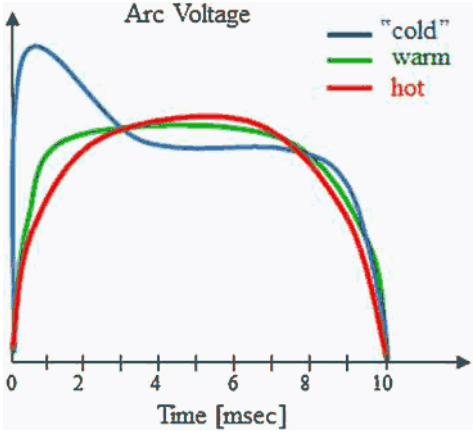

FIGURE 5.13 Qualitative illustration of arc voltage dynamics over a half-period (10 ms) depending on the temperature of the surroundings.

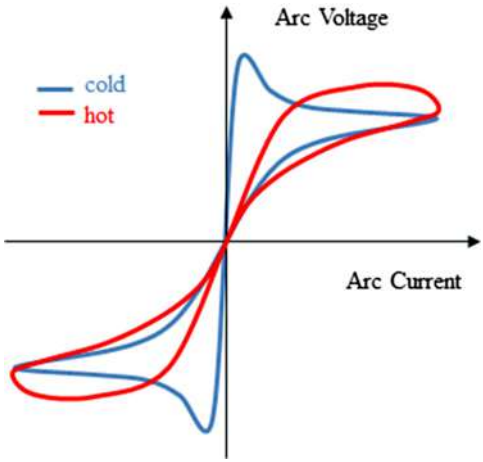

FIGURE 5.14 Qualitative illustration of the dynamic current–voltage characteristics for the case in Figure 5.13 (Lissajous curve).

5.4.2 Electric Arc Models

To understand and predict both the heat transfer from and the electrical characteristics of electric arcs, significant effort has been put into the modeling of electric arcs (Saevarsdottir et al., 2001b). The nature and the level of detail depend mostly on the purpose and application of the modeling. Arc models can be roughly divided into four categories:

1. Momentum source models, where the arc is represented by a momentum source and a heat source included in fluid dynamic reactor models.
2. Black-Box arc models, where attempts are made to simulate the current-voltage dynamics of the arc by fitting parameters on a linear model to

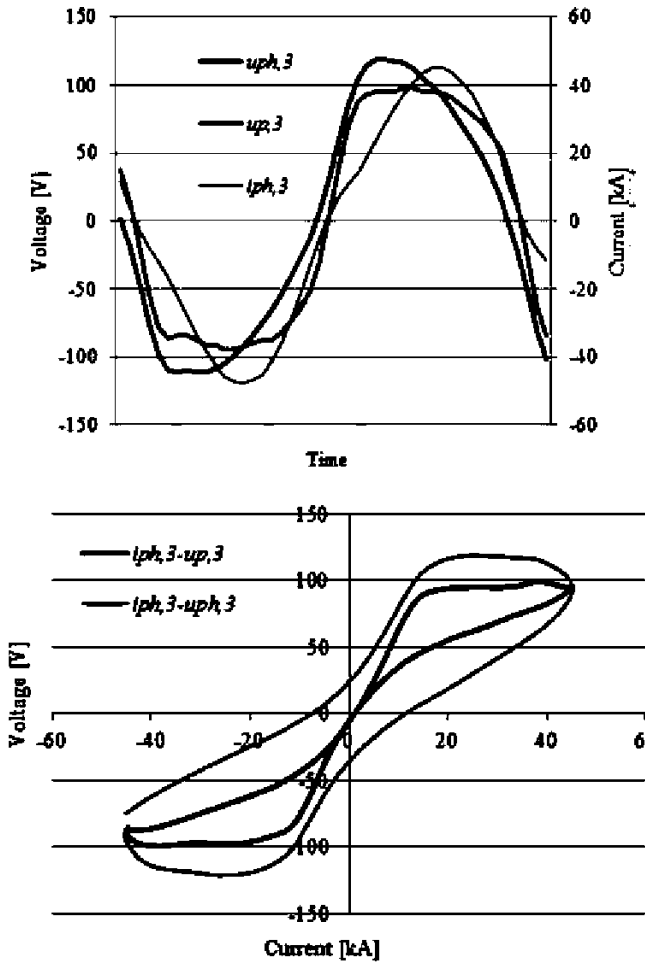

FIGURE 5.15 Current and voltage waveforms for an industrial electric arc in a Si-metal furnace during a period of melting down the charge. A Lissajous curve showing the current voltage relation for an electric arc.

empirical data. No physical justification is required in this category of models. Examples of this type are the Cassie (1939) or Kema arc models.

3. Semiphysical models, where there is a simplified physical view of the arc, based on physical data for plasma properties and the underlying physical phenomena, such as the velocities and radiation.
4. Magneto-hydrodynamic (MHD) models, where the Navier-Stokes equations for energy and impulse balance in the system are coupled with source terms obtained from the Maxwell equations for the electromagnetic fields.

A short description of these respective categories follows. For the purposes of the electric operation of the furnace at the engineering level, the simple black-box approach is probably sufficient, as it does not postulate any specific plasma physics parameters be adopted.

5.4.2.1 Momentum Source Models

In the modeling of arc-heated thermochemical reactors where temperature and flow fields are desired but other arc characteristics are less important, it may be sufficient to replace the arc in the computational domains by a momentum source in the momentum equation and a heat source in the energy equations, which reasonably represents the heat dissipation in the electric arc. An example of this methodology is given by Ravary et al. (2003).

5.4.2.2 Black-Box Models

The so-called phenomenological models were the first type of AC arc models to be established. The purpose of such models is mainly to describe the arc as a nonlinear circuit element when calculating current voltage characteristics. These models are based on very rough assumptions of the physics, and parameters are adjusted empirically. Pioneers in this field were Cassie (1939) and Mayr (1943), but their models were established for circuit breakers. The derivation of the model is based on a rough energy balance, a derivation that results in the following differential equation:

$$R\frac{d}{dt}\left(\frac{1}{R}\right) = \frac{1}{\tau}\left(\frac{u_{arc}i}{P_{arc}} - 1\right) \tag{27}$$

Here the arc resistance R is related to the time constant τ for the arc (which can be derived from the assumed internal energy for the arc), P_{arc} is the power dissipated in the arc, u_{arc} is arc voltage, and i is arc current.

5.4.2.3 Channel Arc Models

A channel arc model (CAM) is a simplified physical model, based on the assumptions that the arc column might be approximated as a conducting cylinder and with a prescribed radial temperature distribution. The cylinder is supposed to have a constant radius R_a apart from a small region at the cathode surface where the arc expands from a cathode spot with a smaller radius R_c (Fig. 5.16). The CAM for AC is based on a DC arc model taken for the condition that at each instant of time the arc strives toward the equilibrium state of the DC arc with the same current. The power dissipated in the arc due to resistive heating in the steady case is equal to the power lost through convection and radiation.

Temperature-dependent physical properties of the arc gas are used to calculate the resistance and other necessary parameters. Convection in the arc is induced by the fluid flow, and the average velocity field for a predetermined

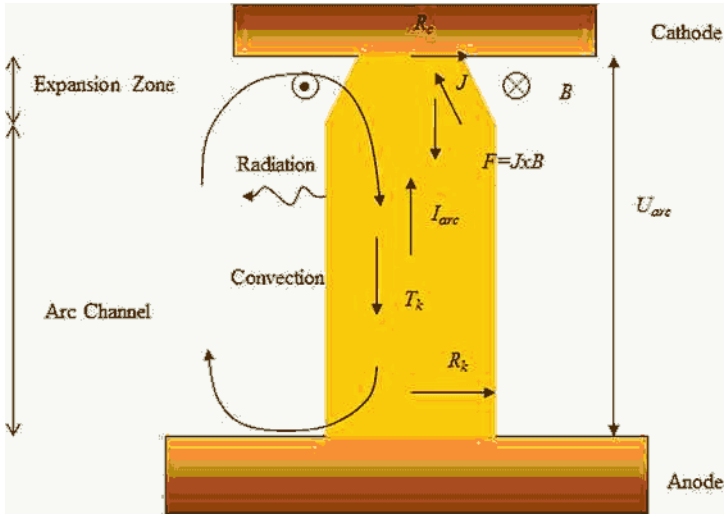

FIGURE 5.16 A schematic illustration of a CAM. *(Based on Saevarsdottir et al., 1999.)*

velocity profile is calculated from the Lorenz force on the current as it expands from the cathode spot into the electric arc channel. The arc temperature and radius have to be chosen such that the energy conservation is satisfied, but there are many values for temperature and radius that would satisfy this requirement. Thus, an additional constraint is imposed, which is that the power dissipation is minimized. This requirement is called Steenbeck's minimum criterion (Steenbeck, 1932). The CAM targets to obtain reasonable arc dynamics using physical principles from a relatively simple model with a small computational time (Larsen, 1996; Saevarsdottir, 2002; Saevarsdottir et al., 1999).

5.4.2.4 MHD Models

This model relies on a magneto-hydrodynamic (MHD) description of the arc behavior. This requires a coupled numerical solution of the Navier-Stokes equation for the conservation of mass, energy, and momentum, with a force term derived from the interaction of the arc current with the magnetic field in the momentum equation, and a heat source term obtained from ohmic dissipation caused by the electric current flowing through the arc. For these source terms, the Maxwell equations must be solved for the magnetic field and current distribution in the arc. The numerical solution procedure requires substantial computational power. In some geometries, the real three-dimensional system might be simplified to two-dimensional-axial symmetry and the problem solved in two dimensions, but important dynamics and instabilities are lost. Reliable time- and pressure-dependent physical data for the operating gas and its composition are required to obtain useful results. For example, a noble gas

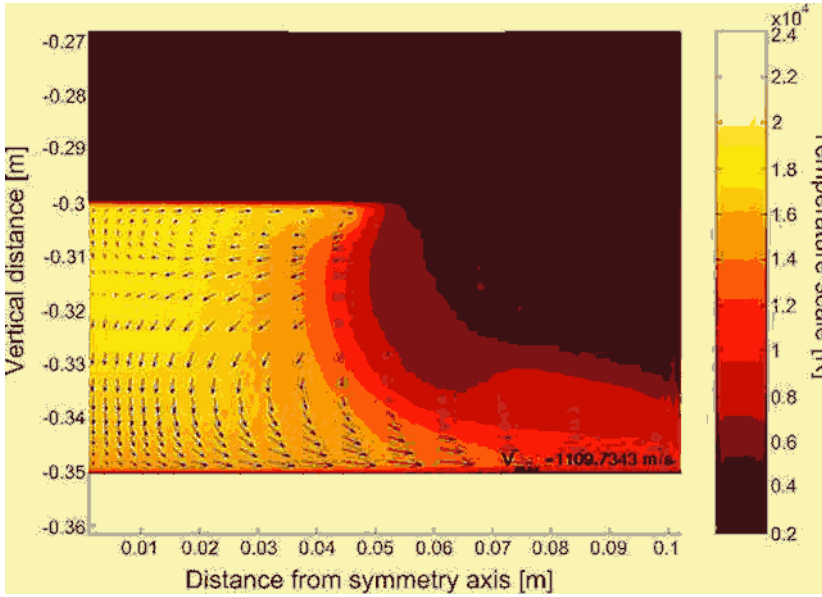

FIGURE 5.17 Temperature and velocity fields from MHD 2D-axisymmetric model for a 5-cm-long arc in SiO:CO 1:1 atmosphere at 100 kA.

like argon (which requires no extra energy for molecular dissociation) will really facilitate arc formation and reduce the nonlinearity of the arc characteristics as compared to air or other di-atomic gases. Thus, the heat required for ionization of argon is much smaller than for molecular gases, and less heat is lost from the arc through convection. Considerable work has been done on MHD modeling of electric arcs, and this clearly gives the most accurate description of the heat transfer and current voltage dynamics for the arc if the model is based on accurate assumptions and physical data. Figure 5.17 shows calculated temperature and velocity fields from an MHD model for a 5-cm-long arc with 100 kA current in a 50% SiO-50% CO atmosphere.

5.4.3 Resistive Heating

As the term *submerged arc furnace* indicates, the top electrodes are submerged in the furnace burden. The burden is composed of a charge of partially reacted and chemically processed raw materials. The initially electrically insulating raw materials in the charge become electrical due to their transformation and melting (Valderhaug, 1992). Electric current passes from the electrodes through the charge to the other electrodes in the furnace in addition to passing through a slag or a coke bed if present in the furnace. Heat is released according to $P_\rho = R_\rho \cdot I^2$. The charge resistivity is different for different

ferroalloy processes and even for the same process it will depend on the charge composition and materials selection (carbon reductant, grain sizes, bulk density, etc.). Direct measurement of the resistivity is also complicated by the variability of the properties depending on the reaction zones within the furnace. Different estimates on the average charge resistivity ρ (in $\Omega \cdot m$) for different processes have been obtained (Downing and Durban, 1966) (Table 5.1). The tabulated resistivity is calculated based on the simplified geometry from Morkramer (1961), so it should be interpreted comparatively rather than exactly.

It is assumed that all conduction happens from the tip of the electrode, which is formed as a half-sphere of diameter d. This is rationalized by a lower conductivity for a less mature charge in the upper zones of the furnace (Morkramer, 1961). The current is assumed to distribute with equal current density in all directions from the half sphere. With a simplifying assumption that the resistivity ρ is uniform in the charge and that the current spreads evenly in the half-sphere to a radius $r >> d$, the phase voltage (the voltage drop from the tip of the electrode to the furnace bottom) would be

$$U_\rho = \frac{\rho \cdot I}{\pi \cdot d}. \tag{28}$$

By measuring the phase voltage and current, the bulk resistivity of the charge may thus be calculated for given electrode diameters.

TABLE 5.1 Estimated Resistivity for Operating Furnace Charge for a Range of Processes

Product	Charge Resistivity ρ [$\Omega \cdot m$]
FeMn standard	0.0020–0.0032
FeSi 75	0.0040–0.0050
FeSi 50	0.0060–0.0085
CaC_2	0.0048–0.0056
Fe	0.0030–0.0060
FeCr with 4–6%C and 2%Si	0.0087–0.0162
FeCr with 4–6%C and 6%Si	0.0050–0.0075
FeCrSi	0.0030–0.0053
SiMn	0.0025–0.0037
P	0.0190–0.0250

5.4.4 Current Paths and Distribution of Heat Dissipation

The main goal of furnace operation is to get good stable operating conditions with a high yield of the produced metal, as well as low energy consumption and as few emissions as possible of dust, harmful gases, and substances. There are many different aspects to furnace operation. Of paramount importance are the selection and feeding of raw materials. The furnace charge must be properly distributed and mixed, through external stoking for an open or semiclosed furnace or by some automatic mechanism of moving the charge in the case of a closed furnace. This will prevent or remedy the eventual segregation of raw materials in the charge, close undesirable vent channels through the charge, and thereby enhance the contact of the process gases with the half-processed raw materials, condensing some gases and enabling reactions with others. Regular and successful tapping of the produced metal from the furnace is also of great importance as metal accumulated in the furnace may reoxidize back to slag under certain conditions.

5.4.4.1 Current Paths in the Furnace

The furnace resistance in an SAF or RHF is controlled by shifting the electrode up and down (Valderhaug, 1992). Lowering the electrode tip further down into the furnace will shorten the current path and improve the electrode contact with hotter and more conducting zones within the furnace, thereby decreasing the phase resistance but avoiding direct submersion into molten metal, as this will lead to a shortcut and electrical breakage. Eventual arcs will also be shorter with lower resistance, which leads to the same result. Raising the electrode has the opposite effect: the current path gets longer, the current will be more evenly distributed through less conductive charge, and there will be less arcing. Therefore, a high electrode holder position will cause higher phase resistance P_ρ, more diffuse and distributed heat dissipation in the furnace, and lower maximum temperatures. For ferroalloy processes where an electric arc is necessary, this may cause an insufficient heat release in the arc itself and therefore an inactive hot zone of the furnace. The consequences are slower reaction rates in the hotter metal-producing regions of the furnace and unfeasible thermodynamic equilibrium conditions leading to loss in metal recovery in the process.

In real furnaces, current distribution paths are, of course, much more complex than assumed in the simplified charge resistance (see Table 5.1). An example of the resistance heating operation mode (an RHF) current distribution is shown in Figure 5.18 for a three-phase AC furnace with a 13-m-wide hearth, 1100-mm self-baking electrodes, and 12 MVA nominal power. This model case includes molten metal, slag, and a coke-rich top layer.

As the model shows, the highest current density is indeed observed around the electrode tip, between the electrodes, and within the molten metal (up to 10^6 A/m^2), whereas close to furnace walls it drops as low as 0.003 A/m^2. One,

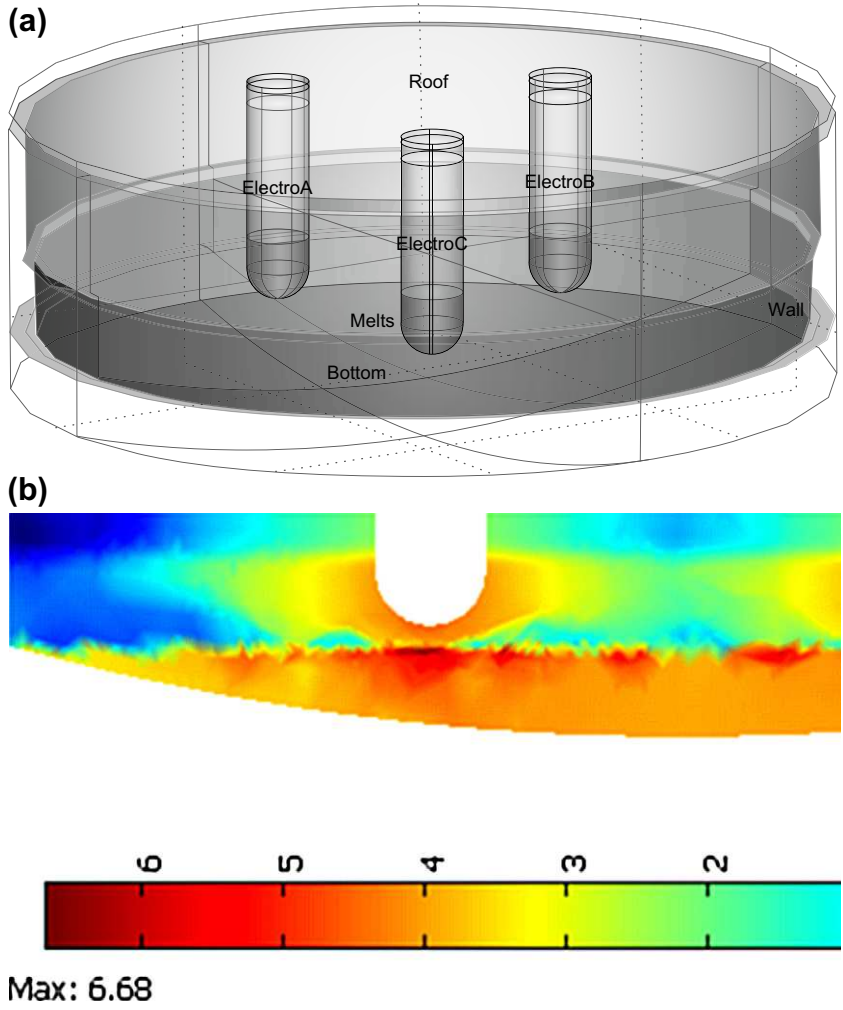

FIGURE 5.18 An example of RHF model geometry (a) and calculated current density distribution (for a cross-section) in logarithmic scale (b), calculated by M. Gasik. Numbers in the color scale are logarithms of the current density in A/m^2.

however, should not make a false conclusion about the heat dissipation in the hearth, as, for example, very high current densities in metal do not necessarily result in excessive heat dissipation because the specific resistance of metal is much lower than that of slag or charge, so active power release there is also low.

5.4.4.2 Heat Distribution in the Presence of an Arc

If the process involves arcing, it can be assumed that the phase current splits up between the charge and the arc. This can be modeled by representing the charge

and arc by their respective resistances connected in parallel with each other and in series to a series resistance as illustrated in Figure 5.19 (Saevarsdottir and Bakken, 2010).

For this phase, the load-bearing operating resistance will then be given by equation

$$R = r + \frac{R_a \cdot R_{ch}}{R_a + R_{ch}}, \tag{29}$$

and the heat dissipation for each location will be in accordance with the magnitude of the resistance. The total active power P for the phase will be the sum of the power released in the arc P_a, in the charge P_{ch} (altogether constituting the useful active power P_ρ in the furnace), and power released in the series short circuit (e.g., electrode) resistance P_s: $P = P_s + P_a + P_{ch}$.

The power released in the charge P_{ch} heats up and melts the charge material and drives endothermic reactions in the upper regions in the furnace. Other heat sources in the area include possible exothermic reactions between process gas and raw materials, oxidation of carbon reductants, condensation of gases, and transfer of thermal energy from the reaction gases passing through.

The arc power P_a is released at T ~20000 K and enables endothermic chemical reactions that require high temperatures to be thermodynamically feasible. It is important to have sufficient temperatures in the high-temperature regions of the furnace to drive the metal generating reactions at a rate that is in balance with other reactions in the furnace that are supported by the charge current heat dissipation and other heat sources.

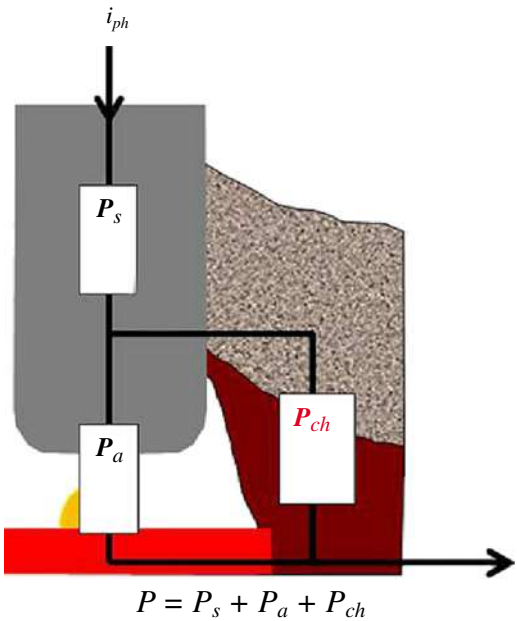

FIGURE 5.19 Equivalent circuit versus crater configuration in the presence of an arc.

The load resistance R_ρ is written as $R_\rho = R_a \cdot R_{ch}/(R_a + R_{ch})$, so P_ρ may be written in terms of R_ρ and the load voltage U_ρ as $P_\rho = {U_\rho}^2/R_\rho$. The charge power P_{ch} and arc power P_a can be found in the same way: $P_{ch} = {U_\rho}^2/R_{ch}$, $P_a = {U_\rho}^2/R_a$. The ratio between the power released in the charge and the total effective power is

$$C = \frac{P_{ch}}{P} = \frac{{U_\rho}^2/R_{ch}}{{U_\rho}^2/R} = \frac{R}{R_{ch}}, \tag{30}$$

which is sometimes called Westly's heat distribution coefficient (Schei et al., 1998). A number of methods have been used in an attempt to evaluate current distribution between arc and charge in furnaces. For example, one method is based on the assumption that the percentage of harmonics in the phase voltage signal was inversely proportional to C. This method applied to a silicon furnace indicates that arc current in a Si furnace is passing by 80% to 90% through the arc. Direct measurements on pilot furnaces and industrial furnaces producing silicon indicate arc current fractions ranging from 30% to 35% up to 50% to 60% (Saevarsdottir and Bakken, 2010; Saevarsdottir et al., 2007).

The heat distribution coefficient C tells the fraction of the electric power dissipated in the charge (Schei et al., 1998), and as discussed previously this fraction should not exceed the maximum for a given process. This enables a balanced furnace operation where the reactions in the different zones run at coordinated rates, so for a particular charge composition with certain conductivity, there is an optimal phase resistance that represents the optimal C value (C_{opt}). If the raw materials in the furnace are changed (and thus electrical resistivity is changed), the overall phase resistance must be adjusted to maintain C_{opt} value. When $C >> C_{opt}$, there is a risk that there will be too little arc current and too much heat dissipation in the charge. That will lead to excessive slag generation in the furnace and reduced metal production. The slag generation will result in bad tapping and reduced sensitivity of the phase resistance to electrode movements as well as excessive consumption of the electrodes along the sides rather than at the tip of the electrodes.

If the operating resistance is lower than the optimal value ($C<C_{opt,}$), the furnace must be run at a higher current to maintain the power load and production rate. This may push electrodes, transformers, bus bars, and other electric equipment beyond the current limits they were designed for, increasing wear and need for extra maintenance. Also, electrode failure risk increases if the phase current exceeds a sensible range.

5.5 ELECTRIC OPERATIONS AND CONTROL OF THE FURNACE

To maintain well-balanced furnace operation and at the same time the optimal and efficient production rate, and high yield for a given furnace design, electric operation is of uttermost importance (Valderhaug, 1992). The power delivered

to the furnace can be controlled by changing the transformer tap positions and by adjusting the electrode holder positions (HPs). Thus, the distribution of power dissipation in the furnace is influenced as discussed previously. Changing the raw materials selectively for electrical purposes can also be seen as electric control, but this is sometimes done in the case of abnormal furnace operation or when the electrode holder position is already too low or high without the target phase current being reached. Another feature that eventually influences the electric operation is the electrode slip control, but over time the slip rate should mainly compensate the electrode consumption.

5.5.1 Power Control

The electric power is fed to the furnace through transformers that normally are connected in the standard Knapsack configuration (see Fig. 5.8). Under special conditions—for example, at startup—the transformers can be connected in a star connection, but under normal operation the Knapsack delta prevails. The transformers convert the high voltage and low current on the primary side to a level fit for the furnace, and the transformer outlet settings determine the voltage level delivered in the delta connection. As the transformer outlet tap positions are adjusted, the power delivered to the furnace changes accordingly as resistance in the furnace is not influenced by this, and current will change with the voltage. Under normal operation, all three transformers have the same settings, providing the furnace with symmetric conditions. Biased settings might occur, but this is not recommended, as it will inevitably lead to circulating unbalanced currents in the delta connections that will not be detected with standard measurements and can lead to equipment failure.

An example of industrial furnace electrical operations is shown in Figure 5.20, which represents a sunflower plot of about 4000 data logs over a month (data analyzed by M. Gasik).

The data shown in Figure 5.20 pertain to the furnace with the geometry and current density distribution shown in Figure 5.18. The furnace is operated for a slag treatment process and the furnace load is targeted for the desirable process temperature range and is therefore operated at a much lower load than its design capacity. As shown, the furnace's active power is proportional to the supplied current that is typical for furnaces operating in resistance mode. The dashed-line ellipse outlines the furnace operational window, but there are also outlying points owing to various causes (shortcuts, charge hanging, improper electrode movement or breakage, external reasons such as maintenance, etc.).

5.5.2 Electrode Control

Assuming that a given voltage is delivered to the delta from the transformers, currents in the furnace are managed by changing phase resistance, which is achieved by controlling the electrode tip position in the furnace. This is done

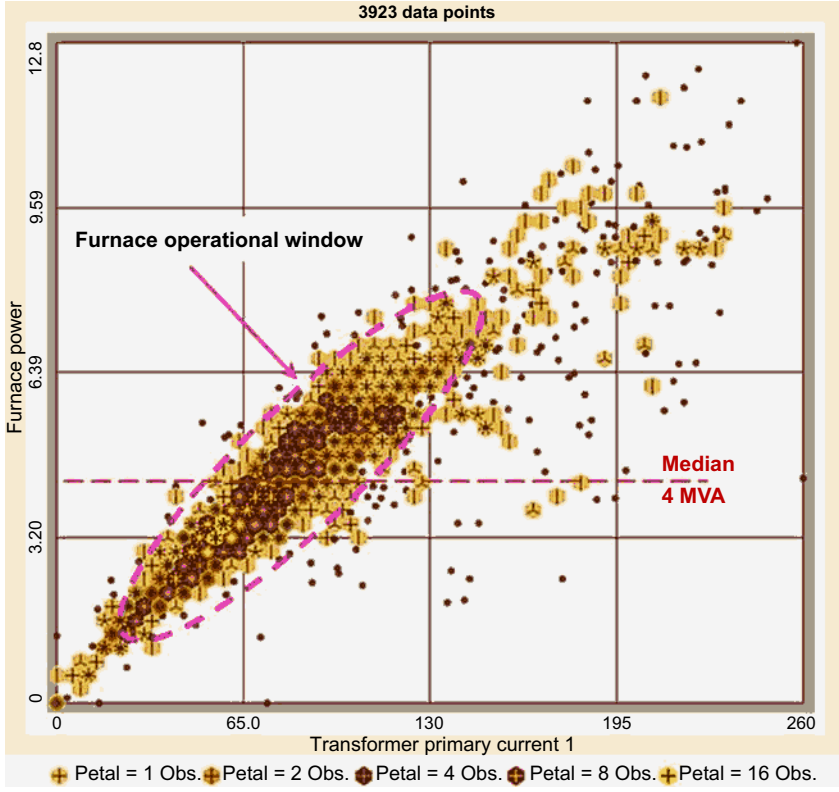

FIGURE 5.20 Data logs of the RHF furnace: power (MVA) versus transformer primary current (A). Each "flower" is a collection of measurements, grouped by number of appearances in this category. The color of the flower and number of petals *(lower legend)* represent how many observations were made at a given set of conditions.

by manipulating the electrode holder positions (HPs) up and down, raising and lowering the phase resistance accordingly. As the phase voltage is more or less determined by the transformer settings, phase current and resistance are interlinked by Ohm's law. There are two strategies for regulating the furnace: resistance regulation and current regulation. Both are based on traditional dead-band regulation. There is a target value for the parameter, a so-called set point, but it is allowed to vary within a predetermined range called a dead band. If the parameter moves out of the dead band range and remains out of limits over a predetermined waiting time, the action of moving the electrode up or down is initiated as illustrated in Figure 5.21. This movement will continue for a certain running time, which is equivalent to a certain displacement of the electrode tip.

In the case of current regulation, there is a target set point for the phase currents, and the dead-band regulation is designed to keep all phase currents

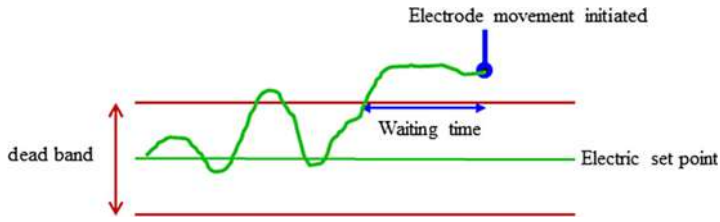

FIGURE 5.21 The concept of dead band regulation, showing the set point, dead band, and waiting time.

within limits. If the current rises above the limit, the electrode is raised to increase the phase resistance and decrease the current. The obstacle is that the change in current in this one phase will influence the currents in the other two phases, through both the floating star point in the furnace and the inductive coupling of the phases. As a consequence, a change in holder position in one phase will be transported to the other phases leading to disturbance in furnace operation, which in the worst case would lead to continuous movement of electrodes, if it is being controlled by automatics. This can be compensated for by using a larger dead band or a decoupling algorithm, but this represents a drawback in this approach to furnace regulation. The level of interaction between the phases depends on the furnace power factor $\cos(\phi)$—the smaller the power factor, the stronger the phase interactions. As the power factor tends to decrease with increasing size of the furnace, this interaction will be more pronounced for large furnaces with a high power load.

The main advantage for the current regulation approach is that the phase current measurement is robust and reliable and done on the primary side of the transformers. Another benefit is that when current is the control parameter, there is less risk for the current to exceed the design limits for the electrode or other equipment. This can be an issue in particular for furnaces that are run at a load exceeding their initial design target value.

The issue of phase coupling can be overcome by regulating directly for the phase resistance rather than the phase current. The resistance is a physical parameter in the furnace, which is not directly influenced by the inductance in the furnace. The complication here is that to determine the phase resistance for the furnace, both the phase current and the phase voltage need to be known. A reliable measurement of the phase current is available, but measuring the phase voltage from the contact clamps to the bottom of the furnace is more complicated. One approach to do this is by using the Bøckmann compensation (Schei et al., 1998), where the voltage drop from the contact clamps to the furnace bottom is measured, and induced currents are compensated for by loop connections (Fig. 5.22).

The weakness of the Bøckmann compensation is that it may not be sufficiently robust for it to be reliable as a control parameter. Some resistance

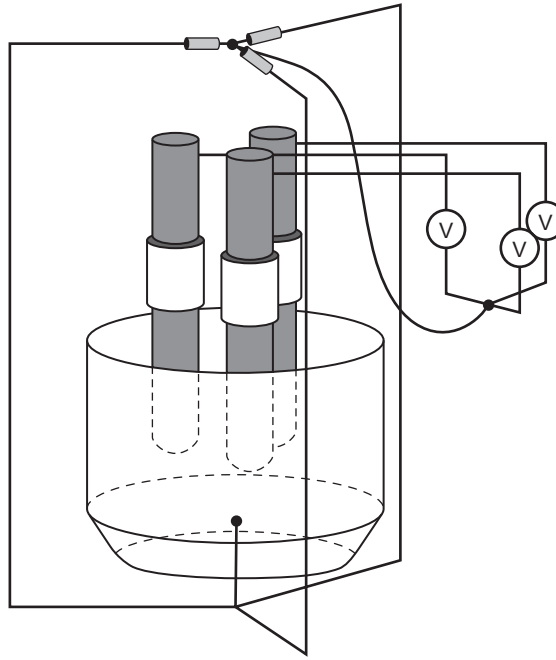

FIGURE 5.22 An illustration of the setup for Bøckmann compensation. *(Modified from Schei et al., 1998.)*

control systems suffice by measuring the contact clamp voltage and use assumptions to deduce a phase voltage. This approach is more robust, but it may be inaccurate in cases when the assumptions are not valid. However, stable operation without the complicating phase interactions has been obtained at a number of smelters that have operated their furnaces with resistance control using this deductive method for evaluating the phase voltage.

An example for the furnace shown in Figure 5.18 and its active power distribution (see Fig. 5.20) can be found in Figure 5.23, which shows the dependence of the phase voltage on the phase current for one electrode (data analyzed by M. Gasik). This sunflower plot represents the same data logs as for active power (see Fig. 5.20) and for the same charge and process type illustrates that when an electrode goes down, resistance drops, and voltage decreases with increasing phase current (solid arrow). The group of the most observations indicates the operational window of this furnace as 65 to 90 V and 20 to 30 kA phase current. When the electrode goes up, resistance increases and so voltage drops, leading to lower current (dashed arrow).

A too-low electrode position (closer to molten metal surface) leads to much higher currents and it indicates to the operator that it might be wise to consider raising the electrode to avoid overheating and possible undesirable short circuits.

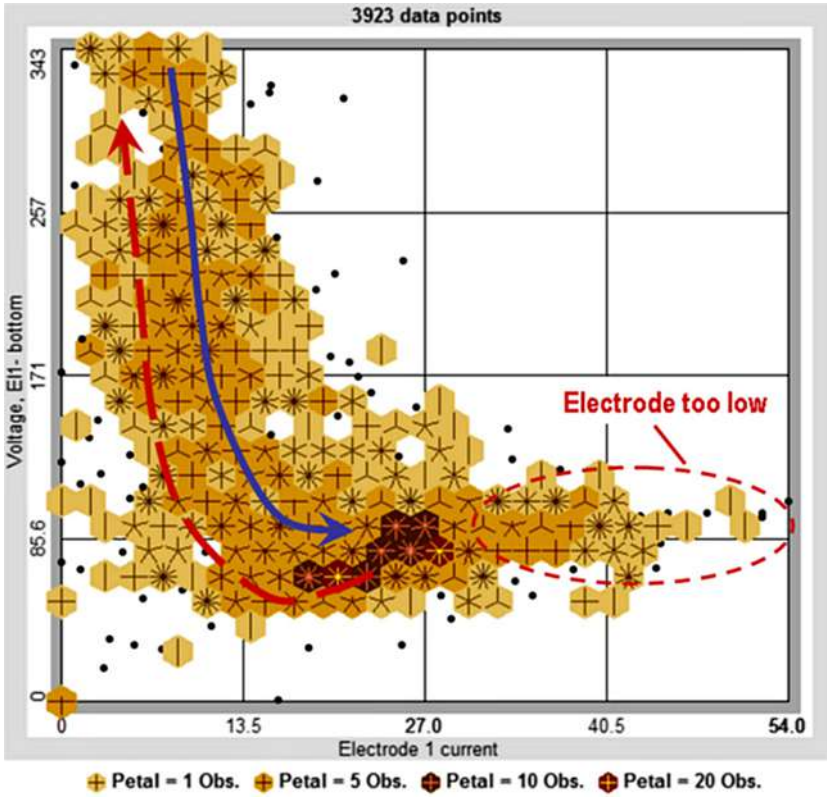

FIGURE 5.23 Data logs of the RHF furnace as one electrode phase voltage (V) versus phase current (kA) for the furnace data shown in Figures 5.18 and 5.20. The blue and red arrows show the lowering and elevation of the electrodes, respectively.

5.6 ENVIRONMENTAL ISSUES OF FERROALLOYS FURNACE OPERATIONS

A number of emissions are associated with ferroalloys production in electric furnaces. The use of modern smokehoods and vents associated with fume treatment makes it possible to substantially reduce most of the harmful emissions and thus the environmental impact of the production facilities, improving the working environment. In this section, various major emissions sources are listed and means of their mitigation discussed.

5.6.1 Particulates Emissions

Particulates are generated by the smelting process in the furnace, tapping, metal refining, and casting. Some dust is also generated during raw material and smelting products storage and handling, preprocessing, crushing, and blending.

The most significant contribution to the production of particulates is the smelting process in the furnace. For example, in silicon and ferrosilicon production, SiO gas from the process burns in oxygen as it mixes with air at the top of the furnace burden, forming amorphous microsilica particles. The microsilica particles are collected in the baghouse filters and are a valuable side product from the process (see Chapter 6 for more details). Also, fine dust in the raw materials is entailed in the gas flow through the charge and carried to the surface. The flue gas from the furnace is drawn through the smoke hood to a duct where the gas must be cooled down before it enters the baghouse filters. The temperature and composition of the gas depends on the extent of enclosure of the furnace. In an open furnace, the gas will be very greatly diluted with air, and therefore a high volumetric flow rate at a moderate temperature will not have a very high dew point due to the dilution. Semiclosed or closed furnaces, on the other hand, will have less dilution, a lower volumetric flow rate in the duct, and higher temperatures. In this case it is more critical to keep the temperature above the acid dew point: due to the presence of SO_2 in the flue, gas acid droplets will form, causing severe corrosion on heat exchange surfaces and damage to the baghouse filter system. An example of sulfuric acid formation conditions is shown in Figure 5.24, versus SO_2 content and gas temperature. It shows that high sulfuric oxide concentrations lead to an increase of sulfuric acid pressure and thus higher dew points.

The heat must be removed from the exhaust gas before it enters the filters, cooling it down to a maximum of ~175°C. Figure 5.25 shows the principle

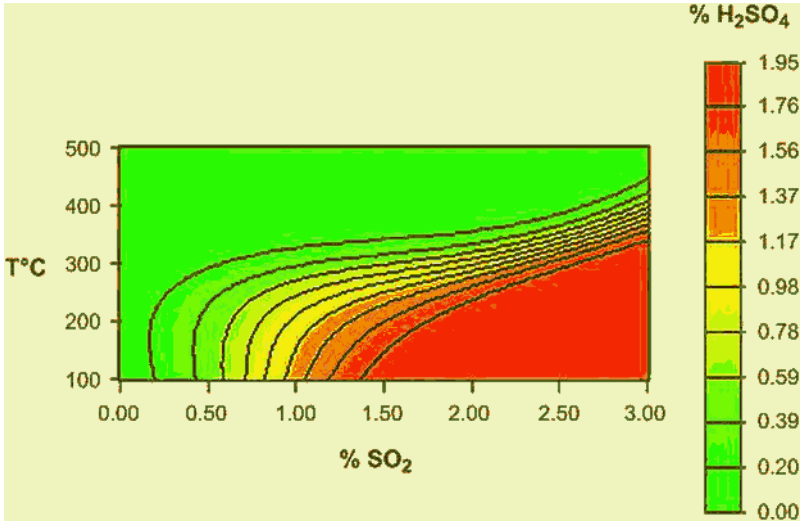

FIGURE 5.24 Approximated sulfuric acid content (vol. %) in a dust-free flue gas (85% CO_2, 4% H_2O, 4% O_2, 0.5% CO, balance N_2) versus SO_2 concentration and gas temperature at cooling. Higher values indicate a more favorable acid mist formation. *(Data provided by M. Gasik.)*

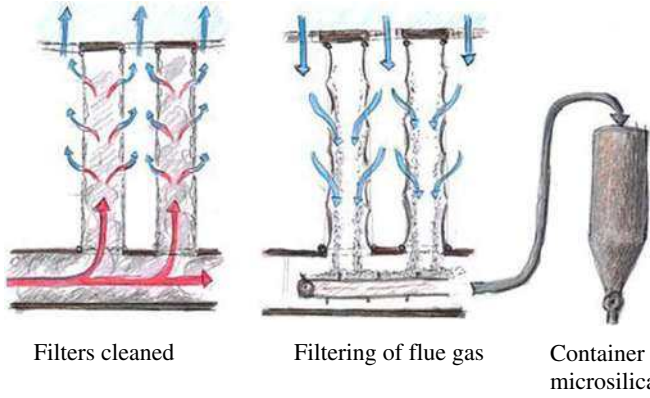

FIGURE 5.25 A schematic drawing of the baghouse filter operation for the removal of microsilica particles from the flue gas from silicon alloy processes. *(Courtesy of Dr. Þorsteinn Hannesson, Elkem Iceland.)*

behind the operation of a baghouse filter system as used in ferroalloy production plants.

During tapping, fumes from the furnace will escape through the tapping hole, burn in the oxygen, and form dust. Ideally, exhaust systems should be installed at the sites where all of these activities take place, removing the dust from the working environment. Figure 5.26 shows the design and operation of a "dog house" smoke vent system located in the tapping area at an Elkem facility.

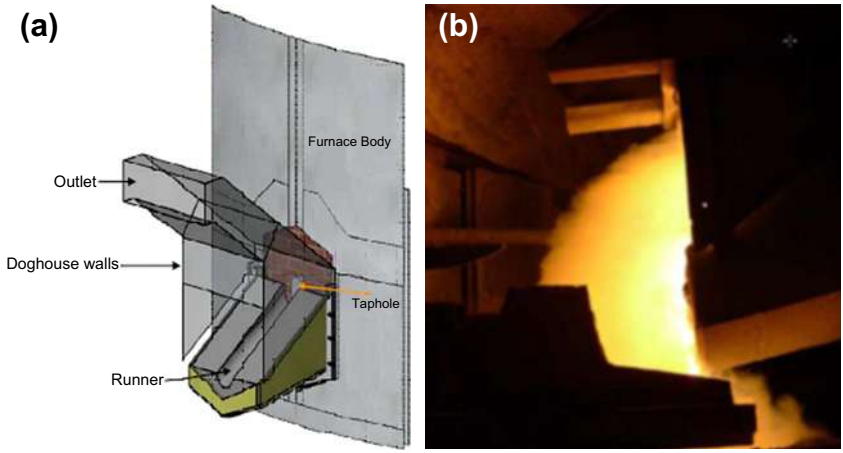

FIGURE 5.26 A schematic (a) and operation (b) of a smoke hood and vent system designed for the tapping area ("dog house") hood installed at an Elkem factory. *(Reproduced with permission from Tveit et al., 2008.)*

TABLE 5.2 Example of Dust Chemical Composition (wt. %) from Some Ferroalloys Smelting Processes

Component	FeSi75…90	Si	FeSiCr	HC FeCr
Fe_2O_3	<0.2	<4	<5	<15
Cr_2O_3	—	—	<1	<5
Al_2O_3	<0.5	<3	<6	5–10
SiO_2	>96	80–96	75–95	15–35
SiC	<1	<4	—	—
CaO	<0.4	<4	<5	<5
MgO	<1	<3	<20	15–25
Carbon	<1.5	<6	<5	3–15
$SO_2 + P_2O_5$	<0.5	<1.5	—	—

In some processes, slags generated in ferroalloy production have high usable metal content and they are recycled so that specific dust collection and handling is not needed. In some other processes where slags are formed with a too-high content of minerals with a high volumetric phase transformation mismatch (e.g., calcium orthosolicate), a self-disintegrating slag is produced, which will cause dust generation as it breaks down. Mitigating means are needed to deal with this issue (Verein Deutscher Ingenieure, 2010). Similar measures should be taken if the metal product is crushed and screened. This will cause the generation of fine dust, which is difficult to collect and recycle. Metallic dust can be highly flammable and should be treated accordingly. Also, an air extraction system should be fitted and ducted to a dust collection device. Table 5.2 summarizes the chemical composition of particulate emissions from a number of ferroalloys smelting processes.

5.6.2 Gaseous Emissions

Ferroalloys production also generates gaseous and vaporous emissions. Most of the emissions originate in the furnace itself. Due to the high process temperatures, various metals may be present in the flue gas, if they have entered the process via raw materials or other sources. The most significant gaseous emission from these processes is sulfur dioxide originating from the carbon raw materials in the process. The concentration in the flue gas depends on the sulfur content in the carbon materials, as well as the level of dilution of the flue gas entering the process. For silicon and FeSi smelting, the common levels of SO_2

in off-gases are below 50 to 60 mg/m^3. Carbon monoxide in the process gases will burn in the presence of air and form carbon dioxide. Also, hydrocarbons from the raw materials will burn to form water and carbon dioxide. Thus, residual CO levels are normally below 30 to 85 mg/m^3.

Due to the high temperatures in the furnace, nitrogen oxides (NOx) are formed both in the furnace and at the tap hole during tapping. Their content might be up to 80 to 120 mg/m^3. There are minor quantities of unburned organic pollutants (Verein Deutscher Ingenieure, 2010) such as benzene, 1.3-butadiene, and PAH, as well as traces of PCB and PCDD/F, which mainly originate from raw carbonaceous materials, carbon-contained charge briquettes, and electrode paste components. Their concentrations in treated waste gas are normally very low, 0.01 to 0.07 mg/m^3. Other pollutants such as nonferrous metals typically are well below 0.001 to 0.010 mg/m^3, as they are normally well captured and recycled.

5.6.3 Heat Emissions and Losses

In ferroalloys production processes, heat is lost in a number of ways. It is removed from the furnace structure, smoke hood, and electrode equipment using cooling water as well as through radiation and convection from the steel lining of the furnace. However, the most significant heat loss stream is the flue gas from the process. For example, in silicon and FeSi production, the energy carried by the flue gas from the furnace is more than the electric energy delivered to the furnace (see Chapter 6), and the temperature in the flue gas, 400° to 700°C, represents a high heat recovery potential (Hjartarson et al., 2010; Schei et al., 1998).

Heat recovery systems for electric power production have been successfully implemented at a number of facilities. The investment and operation is costly and complicated by the amount of dust in the flue gas, which causes severe fouling on heat exchange surfaces, which in turn creates additional maintenance costs. Heat in cooling water from smoke hood and electrode equipment as well as casting equipment can be used as a heat source in applications where low-grade direct heating is desirable, such as in greenhouse cultivation, aquaculture, or district heating with the aid of heat pumps.

REFERENCES

Cassie, A.M., 1939. Theorie nouvelle des arcs de rupture et de la rigitité des circuits. [New theory of breaking arcs and stability of circuits] Proceedings Session on Large Electric Systems, CIGRE Rep. 102, 14 pp.

Chen, F.F., 1990. Introduction to Plasma Physics and Controlled Fusion, Vol. 1: Plasma Physics, second edition. Plenum Press, NY, 421 pp.

Downing, J.H., Durban, L., 1966. Electrical conduction in submerged arc furnaces. Journal of Metals 3, 337–344.

Hjartarson, H., Palsson, H., Saevarsdottir, G., 2010. Waste heat utilization from a submerged arc furnace producing ferrosilicon. Proceedings of Conference INFACON-XII, Helsinki, Finland. 739–748.

Hochrainer, A., 1970. Einige Bemerknungen zum Stromnulldurchgang in Wechselstromschaltern. [Some noticeable loading calculations for the zero crossing in AC switches] Elektrotechnik und Maschinenbau 87, 15–19.

Larsen, H.L., 1996. AC electric arc models for a laboratory setup and a silicon metal furnace. Doctoral Thesis 55. NTNU, Trondheim, 244 pp.

Mayr, O., 1943. Beiträge zur Theorie des statischen und des dynamischen Lichtbogens. [Contributions to the theory of static and dynamic arc] Archives für Elektrotechnik 37, 588–608.

Morkramer, K.L., 1961. Dimensionierungsgrundlagen von Elektro-Reduktionsöfen. [Dimensioning principles of electrical reduction furnace] Elektrowärme 19, 110–116.

Palsson, H., Saevarsdottir, G.A., Jonsson, M.T., Bakken, J.A., 2007. Thermal effects on carbon based electrodes close to a high current electric arc. Proceedings of Conference INFACON-XI, New Dehli, India. 695–702.

Ravary, B., Bakken, J.A., Gonzales-Aguilar, J., Fulcheri, L., 2003. CFD Modeling of a plasma reactor for the production of nano-sized carbon materials. Journal of High-Temperature Material Processes 7, 139–144.

Reynolds, Q.G., 2011. The Dual-electrode DC Arc Furnace – Modeling Insights. Proceedings of the Conference of Southern African Pyrometallurgy 2011, 33–46.

Saevarsdottir, G., 2002. High-current AC arcs in silicon and ferrosilicon furnaces. Doctoral Thesis 56. NTNU, Trondheim, 248 pp.

Saevarsdottir, G., Bakken, J.A., 2010. Current distribution in submerged arc furnaces for silicon metal. Proceedings of the Conference INFACON-XII, Helsinki, Finland. 717–728.

Saevarsdottir, G.A., Bakken, J.A., Sevastyanenco, V.G., Gu, L.P., 2001a. High-power AC arcs in metallurgical furnaces. Journal of High Temperature Material Processes 5, 21–44.

Saevarsdottir, G.A., Bakken, J.A., Sevastyanenco, V.G., Gu, L.P., 2001b. Arc Simulation Model for Three-phase Electrometallurgical Furnaces. Proceedings of the Conference INFACON-9, Quebec, Canada. 253–262.

Saevarsdottir, G., Larsen, H.L., Bakken, J.A., 1999. Modeling of industrial AC arcs. Journal of High- Temperature Material Processes 3, 1–15.

Saevarsdottir, G., Magnusson, T., Bakken, J.A., 2007. Electric arc on a coke bed in a submerged arc furnace. Proceedings of the Conference INFACON-XI, New Delhi, India. 572–582.

Schei, A., Tuset, J.K., Tveit, H., 1998. Production of High-silicon Alloys. Tapir forlag, Trondheim, 63 pp.

Schultz, M.E., 2006. Grob's Basic Electronics, tenth edition. NY: McGraw-Hill, 1286 pp.

Steenbeck, M., 1932. Energetik der Gasentladungen. [Energetics of gas discharges] Physikalische Zeitschrift, 809–815. XXXIII.

Tveit, H., Berget, K.H., Førde Møll, M., 2008. The Silicon Process – The Need for a Major Upgrade of the Internal Environment and Fugitive Emissions. Proceedings of the Conference on Silicon for the Chemical and Solar Industry X, Oslo, Norway. 25–34.

Valderhaug, Aa. M., 1992. Modelling and control of submerged-arc ferrosilicon furnaces. Dr. Ing. Thesis 83. NTNU, Trondheim, 348 pp.

Verein Deutscher Ingenieure, 2010. Emission Control, Carbothermic and Metallothermic Production of Ferroalloys and Silicon Metal. VDI e.V., Dusseldorf, 72 pp.